Exploring the High Temperature AFM *and Its Use for Studies of Polymers*

By: D.A. Ivanov, R. Daniels, S.N. Magonov

Introduction

Atomic force microscopy (AFM) is a well-established surface characterization technique initially introduced for high-resolution surface profiling. Rapid development of AFM instrumentation has significantly extended its capabilities, which now includes measurements of local mechanical, adhesive, magnetic, electric and thermal properties. The spectrum of materials that can be examined by AFM is practically unlimited. Of special interest are studies of soft materials, such as polymers and biological samples, whose mechanical stiffness is comparable, or even much less than the stiffness of commercial AFM probes applied for imaging. This fact allows extraction of structural data from the analysis of these materials at different tip-force levels. For example, low-force imaging is optimal for the correct determination of surface profiles of such samples, whereas imaging at elevated forces can be useful for surface compositional analysis and for recognition of individual components in heterogeneous polymer materials or biological systems[1].

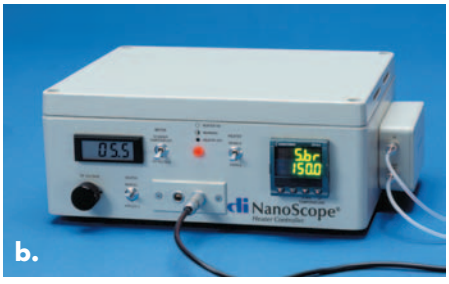

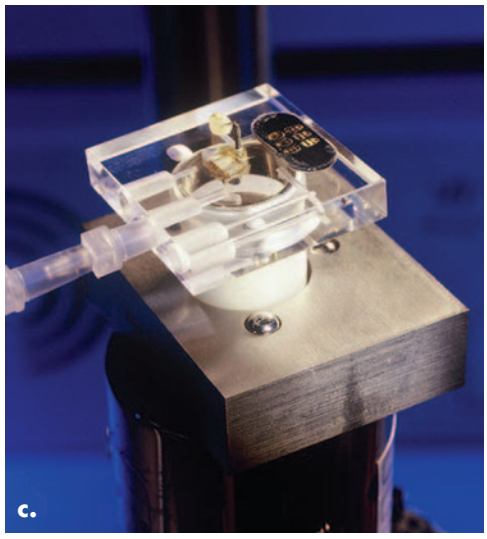

Figure 1. (a) Digital Instruments MultiMode microscope head with the thermal accessory installed; (b) temperature controller; (c) components of the thermal accessory assembled on the piezo-scanner.

Most AFM studies to date have been conducted at ambient temperature. This presents a substantial limitation when information about the thermal behavior of the sample surface is desirable. For example, performance of plastics is strongly temperature-dependent due to their multiple phase transitions, such as melting, crystallization, recrystallization, as well as glass and sub-glass transitions. Experiments illustrating *in-situ* AFM monitoring of polymer crystallization show the unique capability of this technique for measuring the growth of individual crystalline lamellae[2]. This information could not have been obtained with any other microscopic technique. The polymers chosen for the above cited studies undergo crystallization at room temperature (RT); yet the majority of polymers undergo phase transitions above RT. To study these polymers, early experiments were conducted on samples heated

externally for different time periods and then placed on the AFM and examined at RT[3]. This approach is quite laborious since it requires repeated location of the same spot on the sample surface with high precision. In addition, this procedure is not always acceptable because of the changes that can occur in the polymer structure on cooling to RT. Therefore, *in-situ* AFM studies at elevated temperatures are invaluable for analysis of polymers. The work described here illustrates how this can be accomplished with the Digital Instruments MultiMode® AFM[4] equipped with the High Temperature Heater Accessory. A number of important issues relevant for AFM studies at elevated temperatures are addressed. Also several examples of AFM imaging of polymer materials at temperatures up to 250°C are provided.

Historical Background

The importance of AFM measurements at elevated temperatures has been recognized for some time, and several heating stages have been described in other literature[5-8]. By placing a resistive heater (or a Peltier element) guided by a temperature controller on top of the scanner, AFM measurements were performed at temperatures up to 100°C. These first stages were designed for contact mode AFM[5-7], and several examples of imaging under these conditions have been reported[7]. However, contact mode AFM is often problematic for polymer samples because of the strong tip-sample interaction, especially the lateral forces which can cause damage to the sample surface. This problem becomes even more serious at high temperatures. Therefore, the use of TappingMode™, in which the tip-sample contact occurs intermittently without strong lateral force interaction, is necessary for high temperature AFM studies of polymers.

The first heating accessory for the Digital Instruments MultiMode AFM was designed for TappingMode operation at temperatures up to 100°C[8]. In describing this accessory, the authors discussed the need for thermal isolation of the piezo-scanner from the heated sample. To reduce the heat transfer from the sample, a thermal insulating block of balsa wood was applied. This eliminates the risk of the piezo depolarizing and minimizes distortions of the scanner motion caused by the heating of the scanner. The temperature calibration was performed using a thermocouple placed on a piece of Si wafer. The thermocouple reading was in good agreement with the surface temperature of the Si piece measured with Raman spectroscopy. Yet the authors pointed out that this geometry is not identical to that for true imaging conditions when a metallic probe holder is located in the immediate vicinity of the sample surface. It was found that heating the sample to 100°C led to heating of the probe holder to 50°C. They concluded that the thermal balance in the location of the probe can be perturbed by the presence of the holder. Heating of the holder was one of the possible reasons for the drop of the amplitude of the probe, which was driven by a piezo-ceramic stack placed inside the holder. The authors also noticed a linear reduction of the resonant frequency of the Si etched probe with temperature. This required re-tuning of the probe for imaging at different temperatures. Nevertheless, the first step towards AFM studies of polymers at elevated temperatures was made and melting/crystallization experiments were performed on a number of systems[8-9].

Heater Design Considerations

In addition to the issues just discussed, expansion of the temperature range to higher temperatures is obviously desirable. The design of the high temperature heater accessory for the Digital Instruments MultiMode AFM (Figure 1) addresses these issues and provides sample heating up to 250°C. This heater uses the commercial temperature controller "Eurotherm 2216" and a Pt resistive heater. Heating of the sample to the target temperature, defined by the operator, is controlled with feedback from a thermocouple positioned under the sample. In addition to the basic components used in other hot stages, this design includes several features:

- a plug-in sample heater
- a water-cooled scanner
- a probe holder with an additional heater, and
- an environmental enclosure.

The plug-in heater is made of a ceramic and its top contains the Pt resistive heater, a thermocouple, and a small magnet to hold the sample. The heater is mechanically inserted into the top of the scanner. Electric wires, which connect the heating element and thermocouple with the controller, are incorporated inside the cylindrical tube of the piezo-scanner. This plug-in geometry of the heater provides mechanical stability of the heater's contact with the scanner and avoids mechanical interference from any external connections (e.g. wires) to the heater during scanning. The top part of the piezo-scanner includes a small reservoir where the cooling water circulates. The water is driven from an outside pool by a peristaltic pump and efficiently reduces the heat transfer to the scanner. With this design, the temperature of the scanner never

exceeds 45°C at a sample temperature of 250°C, which ensures stable performance.

To enhance the stability of the probe oscillations, the probe holder used in the high temperature accessory is made of fused silica and contains a heating element for the AFM probe. Amplitude of the oscillating probe can substantially change with temperature because heating of the probe holder influences mechanical coupling between the probe and the holder. However, for most applications this is not a concern because the amplitude can be brought to a desired magnitude by varying the amplitude of the driving signal applied to the piezo-stack. The holder together with a rubbery silicone seal forms a gas-tight enclosure for the sample, which can be used to create controlled atmosphere conditions. For example, inert gas purging can be necessary to avoid oxidative degradation of samples at high temperatures. The function of the probe heater and the environment control is described in more detail.

From the first AFM studies at elevated temperatures, it became clear that Si etched probes without any coating are preferred for such measurements. Coated probes can bend and/or twist at elevated temperatures. It has also been found that water condensation occurs when operating in TappingMode at medium and high temperatures. When the sample temperature approaches 100°C and the probe is slightly colder, water condensation in the form of small droplets is typically observed on the probe's backside. In some cases, the volatile components of the heated sample can also cause the droplet formation. Heating of the probe was implemented to avoid this problem[10]. By placing a heater close to the probe

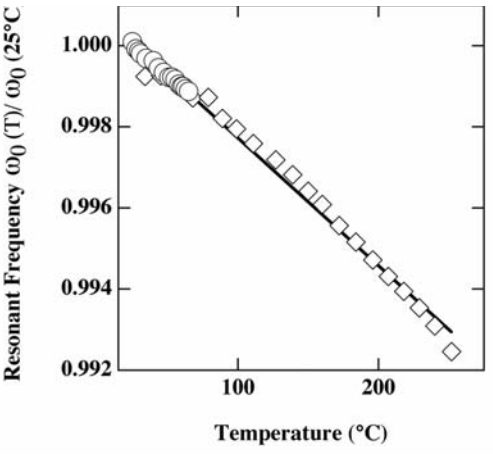

Figure 2. Temperature dependence of the resonant frequency of a Si cantilever. Symbols: circles are the data obtained with the Digital Instruments MultiMode AFM; squares are the data recalculated from the temperature dependence of the elastic modulus of Si (100)[14]. Solid line presents a linear fit to both sets of data.

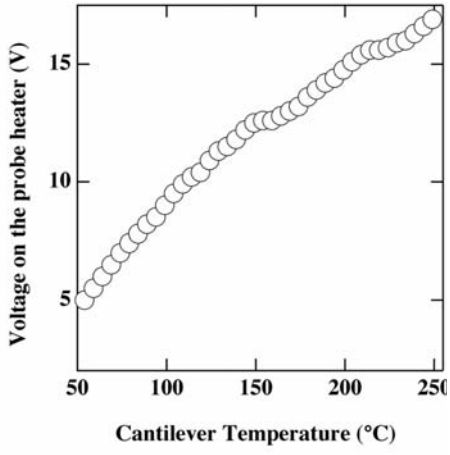

Figure 3. Relationship between the voltage applied to the probe heater and the probe temperature. The probe was located within 5μm of the sample surface heated to the same temperature.

mount it became possible to change the probe temperature by regulating the voltage on the heater. In this case, heating of the probe and the probe holder assembly to the target temperature also induces heating of the sample from above, which can significantly improve the homogeneity of the temperature distribution throughout the sample. This dual heating is of particular importance for thicker samples and for materials with low heat conductivity.

In order to quantify and control the probe temperature and the conditions of imaging, accurate measurement of the probe temperature is required. To determine the temperature of the probe itself, we use the resonant frequency of the probe as a measure of its temperature. The angular resonant frequency of a rectangular lever without a concentrated load is given by[11]

$$\omega_0 = \frac{t}{l^2}\sqrt{\frac{E}{\rho}}$$

where t and l denote the thickness and length of the lever, E the elastic modulus and ρ the mass density. The variation of ω_0 with temperature can be accounted for by the thermal expansion of the lever and by the temperature variation of the elastic modulus. However, for the single crystalline silicon material of the TappingMode probes in the temperature range of our measurements, the latter contribution dominates. Thus one obtains

$$\frac{\omega_0(T)}{\omega_0(T_0)} = \sqrt{\frac{ET}{ET_0}}$$

where T_0 denotes some reference temperature (in our case T_0 = 25°C). To correctly determine the thermal variation of the cantilever resonant frequency, we placed the head of a Digital Instruments MultiMode AFM into an oven and recorded the resonant frequency of the Si probe as a function of temperature[12]. The results of these measurements are given in Figure 2. On the same graph, we plot the values of the resonant frequency recalculated from the recent literature data[13] on the temperature dependence of the elastic modulus of Si[14]. Notice that the resonant frequency is changing

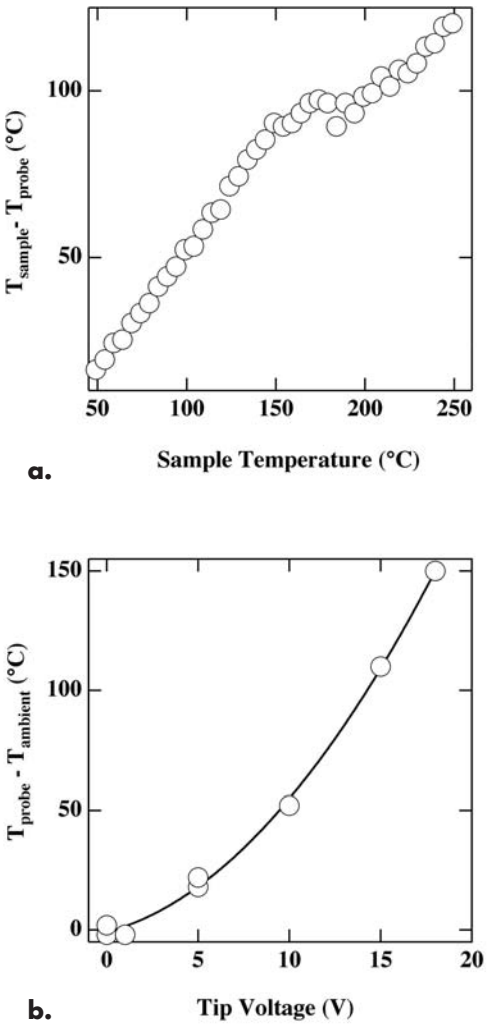

Figure 4. (a) Difference between the temperature of the sample and the probe at different sample temperatures; (b) relationship between the voltage applied to the probe heater and the probe temperature.

almost linearly with temperature between 25°C and 250°C. In addition, the frequency-versus-temperature results correlate well with the literature data obtained with a similar AFM probe[8]. The average coefficient of $3.1 \times 10^{-5} \pm 5 \times 10^{-7}$ °C^{-1} describes the relative decrease of the cantilever resonant frequency with temperature. For Si etched probes (225µm long and 30-40µm wide, with a stiffness ~40 N/m) this variation results in ~5.2 Hz/°C.

Next, we used the calculated resonant frequency-versus-temperature relationship to generate the thermal equilibrium conditions at the sample location under the AFM probe. To achieve this, the voltage applied to the probe heater is chosen from the curve (Figure 3) such that the temperature of the probe matches that of the sample. By contrast, if the probe heater is *not* activated, the temperatures of the sample and the probe can differ substantially (Figure 4a). Similarly, by applying the voltage to the probe heater while the sample heater is off, one can locally change the temperature of the surface underneath the probe. The corresponding dependence between the probe temperature and the voltage (V) is shown in Figure 4b. It can be seen that the temperature difference (ΔT) scales as the square of the voltage, which is logical since the heat flux released by the heater is proportional to V^2 and the heat exchange between the probe and its surroundings is proportional to ΔT.

This separate control of the sample and probe temperatures opens the way to perform well-defined *in-situ* thermal treatments. With polymers, the thermal history (heating and cooling rates) is important in defining the final morphology. The maximum heating rate provided by the sample heater is up to 50°C/min, as measured with a thermocouple underneath the sample. In order to evaluate the maximum attainable heating and cooling rates of the probe, we applied a specially designed electronic set-up for tracking the cantilever resonant frequency and performing data acquisition at one sample per second. The corresponding results given in Figure 5 show that the heating and cooling rates of the probe can be extraordinarily high. The heating rate of the probe when the temperature was brought from 100 to 200-250°C reached 960°C/min; the corresponding cooling rate attained values as high as 600°C/min. These heating rates at the surface are much higher than are obtainable with other methods. Obviously, the heating rate of the bulk sample with this accessory will be much less than that of the probe, allowing studies of differential localized heating and cooling at the surface of the sample.

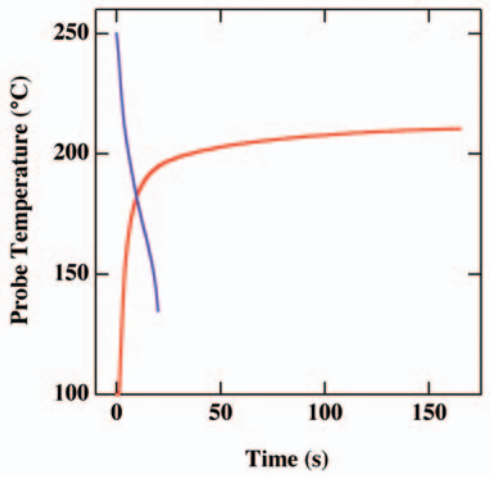

Figure 5. Time dependencies of the probe temperature after stepwise changes of the voltage applied to the probe heater. Red line corresponds to the probe heating after the jump from 9.1 to 17.0V. Blue line corresponds to the probe cooling after the voltage was decreased from 14.8 to 9.1V.

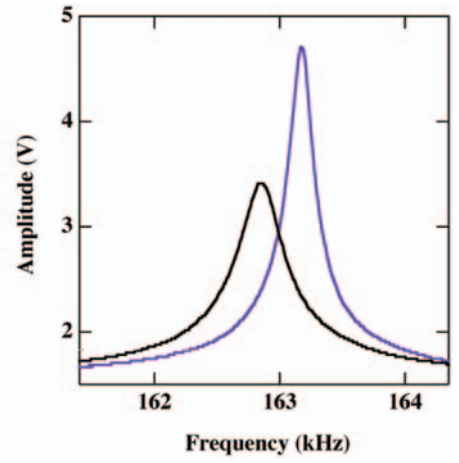

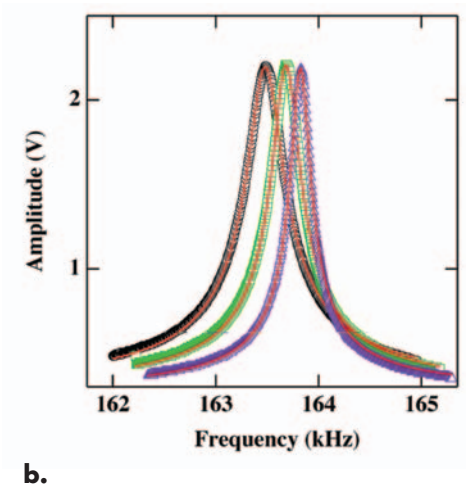

Figure 6. (a) Amplitude-versus-frequency curves obtained in air (black line) and in He (purple line); (b) amplitude-versus-frequency curves after re-tuning in air (black curve), in the sample environment partially filled with He (the rubber seal was not installed, green curve) and in He environment (the rubber seal was installed, purple curve). The red solid lines correspond to the fits of the data to the approximate expression (equation three in reference twelve). The quality factors calculated from the fits are 494, 632 and 910 for the black, green and purple curves, respectively.

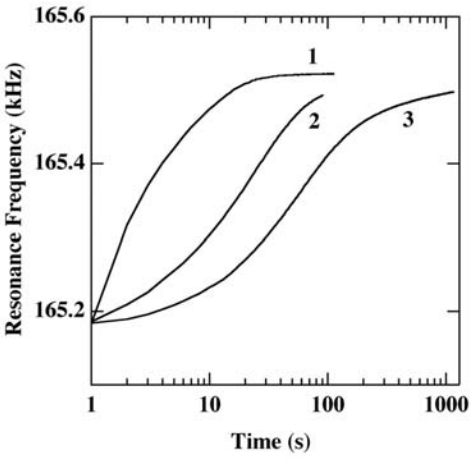

Figure 7. Time dependencies of the probe resonant frequency in the environmental sample enclosure during purging of He at 40 (1), 10 (2) and 4 ml/min (3) purging rates.

As mentioned, environmental control is a necessary requirement for high temperature AFM measurements of polymers. Helium atmosphere is recommended because of the high sensitivity of the oscillating probe to the air-to-He exchange. Higher resonant frequency and a larger quality factor characterize the probe oscillation in He (Figures 6 a-b) as compared to air. It is worth noting that the silicon rubber seal is required for better gas exchange (Figure 6b). Monitoring the cantilever resonant frequency after the purging starts allows estimation of the rate and the extent of the gas exchange in the sample environment (Figure 7). The gas exchange is complete in 20 seconds at a purging rate of 40 ml/min. Lower purging rates can increase the equilibration time.

In practice, high temperature AFM imaging of polymer samples shares many similarities with imaging at RT. Small sample size ensures better conditions for fast heating and equilibration of the sample temperature. Polymer films and small polymer blocks (with a top surface prepared with an ultramicrotome), which are placed on a metal puck (6mm in diameter) have been routinely examined with the heater accessory. During sample heating the probe is disengaged from the sample and the driving frequency is re-tuned at each temperature. For imaging of polymers close to their melting points it is generally preferable to use larger oscillating amplitudes of the probe in order to overcome the adhesive tip-sample interactions.

Practical Examples

To illustrate application of the heater accessory to polymers, we have chosen several examples showing the most important performance features: sub-micron imaging in a broad temperature range and the ability to monitor structural changes at the same surface location. The first example is taken from AFM studies of self-organization of polymers with mini-dendritic side groups on graphite. These macromolecules with side alkyl chains exhibit epitaxial order on graphite. The images of the samples prepared by spin casting from very dilute solutions on graphite reveal individual macromolecules in extended-chain conformation that allow quantification of their molecular weight[15]. It is important to follow the process of polymer chain ordering on graphite, which occurs after their spin casting[16]. The AFM image, which was obtained on the sample immediately after it was spin cast,

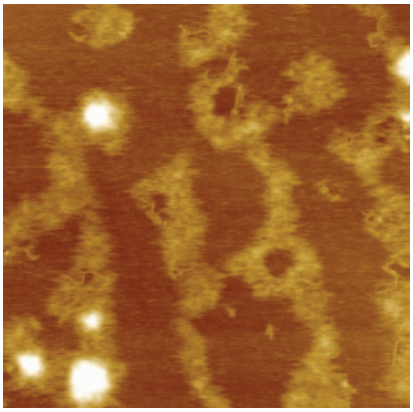

a. *1μm T=30°C*

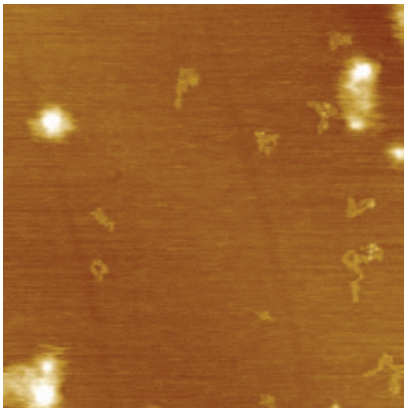

b. *1μm T=50°C*

Figure 8. (a-b) Height images of samples prepared by spin casting of a dilute solution of a polymer with mini-dendritic blocks (see the chemical structure below) on graphite.

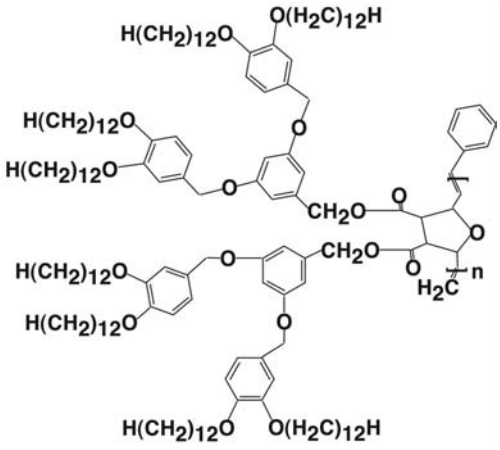

shows small aggregates formed by a few macromolecules, which are hidden amidst patches of non-ordered material (Figure 8a). These patches disappeared after heating of the sample to 50°C, indicating that they are most likely of low molecular weight (Figure 8b). With increasing temperature, the mobility of the chains increases and their attachment to graphite loosens. As a result, the AFM probe can easily displace them from the surface; thus the single macromolecules are no longer seen at temperatures above 75°C and only thick islands are found[16]. At these temperatures, the displaced polymer material, most likely floats in a liquid overlayer, which is often present on surfaces at ambient conditions. When the sample temperature was lowered to RT, the polymer chains re-attach to the substrate again. Two kinds of domains – thin and thick – are seen in the images recorded at RT (Figure 9a). Single layer domains, which exhibit well-ordered macromolecular arrangement, surround the thicker domains (Figure 9b). In the layer lying directly on the graphite, cylindrical-shaped macromolecules are aligned along the main axes of the substrate and, therefore, the chains fold at regular angles of 60 and 120 degrees. After the sample was heated to 150°C, only thick domains were observed (Figure 9c). One of the three thick domains seen at RT has disappeared and the other two have become larger. This observation indicates that some transfer of material has been assisted by the AFM probe at these high temperatures.

The second example shows morphologic changes observed in a thin film of syndiotactic polypropylene

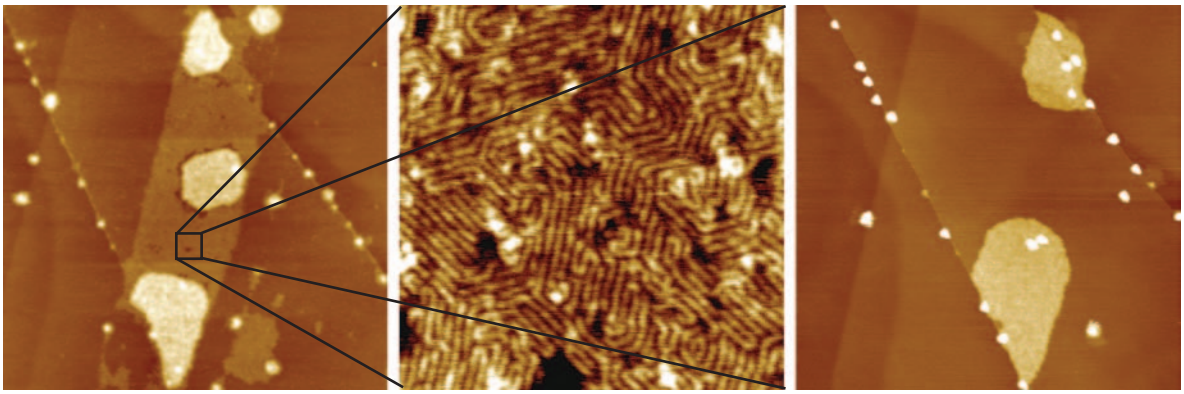

a. *3μm T=30°C* **b.** *250nm T=30°C* **c.** *3μm T=150°C*

Figure 9. (a,c) Height images of the samples prepared by spin casting of polymer solution with mini-dendritic blocks on graphite. Images were taken at different temperatures. (b) Height image of the smaller area, shown in box in (a).

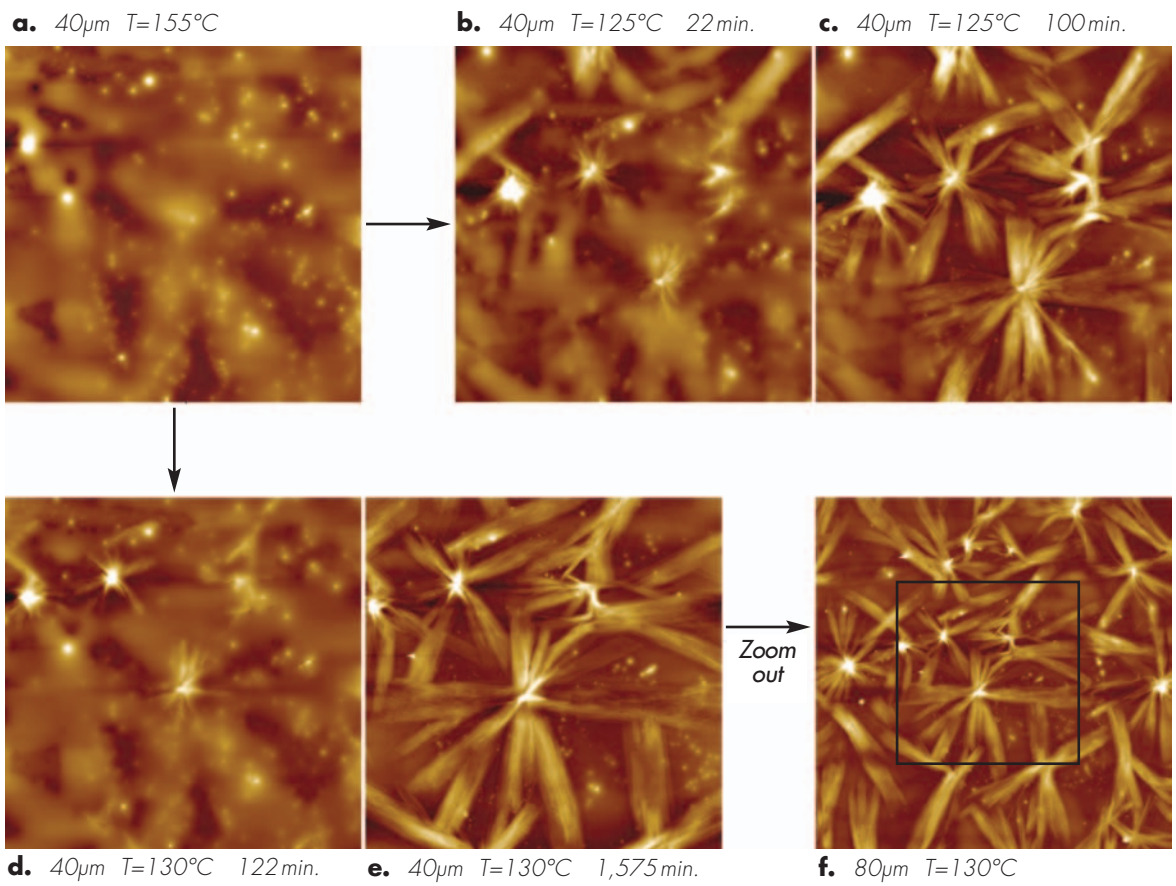

Figure 10. (a-f) Height images of syndiotactic polypropylene (sPP) film at different temperatures. (a) Image of the sPP melt. Images in (b) and (c) were obtained during crystallization at 125°C for periods indicated above the images. Images in (d) and (e) were obtained during crystallization at 130°C. Image in (f) shows the final morphology after crystallization at 130°C in the area surrounding the location shown in (d) and (e).

(sPP) upon crystallization at two different temperatures, 125°C and 130°C. A featureless area is seen in the image in Figure 10a, representing the surface of sPP in the melt when the sample temperature is around 155°C. After the sample temperature is lowered to 125°C, polymer crystallization proceeds with formation of spherulite-like morphology. The series of images in Figure 10b-e demonstrates the capability of monitoring polymer crystallization at the same location at different temperatures. The polymer crystallization is substantially slower at higher temperatures (T=130°C), yet the final crystalline morphology with spherulite-like structures does not vary much for these temperatures. The flat on lying lamellae, which grew from centers of the spherulites, resemble single crystal sPP platelets. Additional AFM results, which reveal morphologic and nanostructural changes during melting and crystallization of single sPP crystals, are published in Macromolecules[17].

In *in-situ* AFM studies of polymer crystallization, one should be aware that crystallization can be induced by the tip-sample interaction during repeated imaging of the same sample area. A simple check on these tip-induced effects consists of later scanning of a larger area that includes the area scanned during the experiments. For example, the image in Figure 10f shows an 80μm scan of the sPP sample, which exhibits similar crystalline morphology over the entire area, regardless of where previous scannng occurred during crystallization. This result indicates that the probe has not caused morphological modification of the surface.

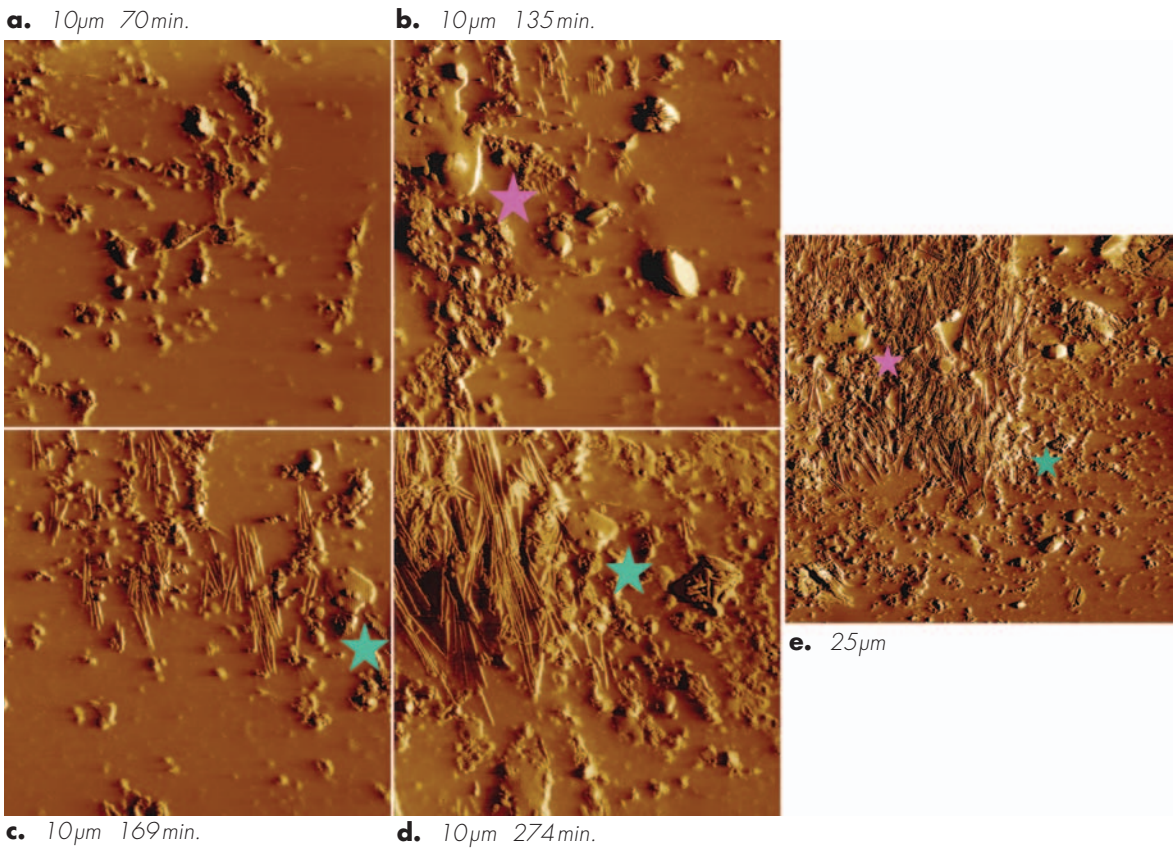

Figure 11. (a-d) Phase images obtained during crystallization of isotactic polypropylene at 140°C for different times. (e) Phase image showing a larger area of the sample including the location where the crystallization proceeded most efficiently (top left corner). Colored stars indicate the same place in the respective images.

Conversely, Figure 11 demonstrates the acceleration of polymer crystallization due to the probe, which was colder than the sample. After melting of a relatively thick (0.5mm) block of isotactic polypropylene (iPP) at 150°C, the temperature was decreased to 140°C, and morphologic changes accompanying polymer crystallization were monitored in the 10μm area. Due to the high temperature, this process was relatively slow. The first indications of polymer crystallization appeared after one hour, and several flat on and edge-on oriented lamellae were recorded after two hours (Figures 11a-b). Further progressive growth of lamellar aggregates, which was monitored at a neighboring 10μm location, is demonstrated in Figures 11c-d. Thermal flow of this sample (most likely due to its substantial thickness) was more pronounced compared to other examples. Yet the flat on lamellae relevant to both locations can be seen in the larger-scale image in Figure 11e. In Figure 11b-e the lamellae are marked with differently colored stars. The large-scale image (Figure 11e) also reveals that crystallization was much faster in the area where the imaging was performed. This area in the left top corner of the image in Figure 11e is completely covered by lamellae. During this experiment, the voltage applied to the probe heater was 10V. This value is lower than needed to achieve 140°C (see graph in Figure 3). We conclude that the tip and, therefore, the surface location under the probe, were colder than the surrounding material, and this accelerated the polymer crystallization.

The last example demonstrates the ability of AFM to monitor polymer crystallization at temperatures well above 200°C. Three snapshots of the real time melt-crystallization of poly(ethylene terephthalate), or PET, at 230°C are presented in Figure 12. It is important to emphasize that we were able to monitor high temperature PET crystallization by performing imaging at the same location with sub-micron resolution. Notice the appearance of individual crystalline lamellae (approximately 9nm in width), and their growth and pronounced tendency to

form stacks. The arrows in Figure 12 indicate the same locations on the sample surface where the growth proceeds via stack thickening, i.e. via increasing the number of lamellae per stack. These stacks eventually form a space filling crystalline structure.

Despite the fact that PET, a typical aromatic polyester with semi rigid chains, has been intensively studied for many years, direct microscopic observation of its structure and evolution at the nanometer scale had not yet been achieved[18]. Visualization of PET's sub-micron organization, which is now possible with AFM at elevated temperatures, offers new insights into the lamellar structure and crystallization behavior of this polymer[19]. These insights can also help to correctly interpret SAXS (small angle X-ray scattering) data using the direct-space information obtained by AFM. In particular, one can readily see from the AFM images in Figure 12 that the crystalline lamellae of PET are thinner than the interlamellar amorphous layers. Finally, the X-ray data can be quantitatively compared with AFM data by performing a reciprocal-space treatment of AFM images, as described elsewhere[20].

Conclusions

The described High Temperature Heater Accessory for the Digital Instruments MultiMode AFM meets the strong demand for AFM measurements at elevated temperatures. The accessory accommodates several new features: probe heater, water-cooled scanner and environmental control for ensuring stable imaging of samples at temperatures up to 250°C. The practical examples selected for this work demonstrate the capabilities of high temperature AFM studies with this accessory. Several other applications, which were accomplished using different prototypes of the heating stage, were reported earlier[20,21]. We believe that a broader use of this accessory for AFM applications to polymers will bring invaluable information for academic and industrial researchers.

Acknowledgements

The authors are thankful to their colleagues at Veeco Instruments Inc.: Russ Mead for his contribution in converting the prototype of the heating accessory to the final product, Karl Koski for his fine mechanical work in assembling sample heaters and other components of the accessory, and Monte Heaton for reviewing and editing the manuscript. The authors are grateful to Zhor Amalou (Universite Libre de Bruxelles) for preparation of a PET sample and also to N. Ono (Mitsubishi Materials Corp., Silicon Research Center) for kindly providing the numerical data on the temperature dependence of the elastic modulus of Si. D.A. Ivanov is thankful to Veeco Instruments Inc. for the support of his stay in Santa Barbara, where this research work was accomplished.

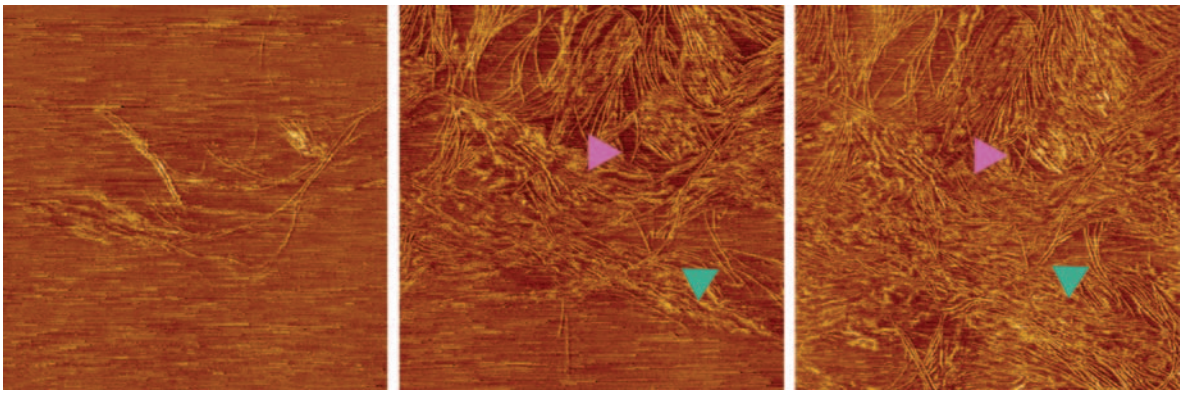

a. *3μm T=230°C* **b.** *3μm T=230°C* **c.** *3μm T=230°C*

Figure 12. Phase images showing the growth of crystalline lamellae during the melt-crystallization of poly(ethylene terephthalate) at 230°C; the images were taken at the same location. The arrows indicate the places where the crystal growth proceeds via the stack thickening mechanism.

References

1. For recent reviews, see S.N. Magonov "Atomic force microscopy in analysis of polymers" in "Encyclopedia of Analytical Chemistry", R.A. Myers (Ed.), pp. 7432-7491, Wiley & Sons, Chichester, 2000; V.J. Morris, A.R. Kirby, A.P. Gunning "Atomic force microscopy for biologists", World Scientific Publishing, Singapore, 1999.
2. T.J. McMaster, J.K. Hobbs, P.J. Barham, M.J. Miles, AFM Study of *in-situ* Real Time Polymer Crystallization and Spherulite Structure, Probe Microscopy 1, 43. (1997); "Direct Observation of Growth of Lamellae and Spherulites of a Semicrystalline Polymer by AFM" Lin Li, Chi-Ming Chan, King Lun Yeung, Jian-Xiong Li, Kai-Mo Ng, Yuguo Lei, Macromolecules, 2001, in press
3. D.A. Ivanov, A.M. Jonas "Isothermal growth and reorganization upon heating of a single poly(aryl-ether-ether-ketone) (PEEK) spherulite, as imaged by atomic force microscopy", Macromolecules, 1998, 31, 4546-4550.
4. With the MultiMode AFM, the sample is placed on the top of the scanner and imaging is performed by rastering the sample underneath an immobile probe. In other SPM microscopes, e.g. Dimension Series, the probe is attached to the scanner and it is moved over the fixed sample surface.
5. I. Musevic, G. Slak, R. Blinc, "Temperature controlled microstage for an atomic force microscope" Rev. Sci. Instrum. 67, 2554 (1996)
6. T.R. Baekmark, T. Bjornholm, O.G. Mouritsen, "Design and construction of a heat stage for investigations of samples by atomic force microscopy above ambient temperatures" Rev. Sci. Instrum. 1997, 68, 140.
7. H.D. Sikes, D.K. Schwartz "Two-Dimensional Melting of an Anisotropic Crystal Observed at the Molecular Level" Science 1997, 278, 1604-1607.
8. S.G. Prillman, A.M. Kavanagh, E.C. Scher, S.T. Robertson, K.S. Hwang, V.L. Colvin "An *in-situ* hot stage for temperature-dependent tapping mode atomic force microscope" Rev. Sci. Instrum. 1998, 69, 3245-3250.
9. R. Pearce, G.J. Vancso, "Real time imaging of melting and crystallization in poly(ethylene oxide) by atomic force microscopy" Polymer 1998, 39, 1237-1242.
10. R. Daniels, S.N. Magonov "Method and system for increasing the accuracy of a probe-based instrument measuring a heated sample", US Patent Application No 09/354,448, 15 July 1999.
11. D. Sarid "Scanning force microscopy with applications to electric, magnetic, and atomic forces'', Oxford University Press, 1991.
12. It should be noted however that the value that we are measuring in ambient conditions with an AFM cantilever is not strictly equal to $d\omega_0/dT$. Indeed, already in a very simple model of the forced damped oscillator the resonant frequency (ω_r) and ω_o are slightly offset [Fowles, Grant R. "Analytical Mechanics", Saunders Golden Sunburst Series, 1986]: $\omega_r = \sqrt{\omega_0^2 - 2\gamma^2}$

    where γ denotes the dissipation term in the differential equation of the cantilever motion. Thus the presence of damping somewhat slows down the oscillator. The dissipation term γ can be related to the quality factor (Q) of the oscillator as $Q = \frac{\sqrt{\omega_0^2 - \gamma^2}}{2\gamma}$

    We have calculated the values of Q by fitting the amplitude of the cantilever oscillation as a function of frequency to the standard approximate expression

    $$A(\omega) = \frac{A_{max}\,\omega_o}{\sqrt{4Q^2(\omega_o - \omega)^2 + \omega_o^2}} \quad (3).$$

    It was found that Q does not change significantly in all the temperature range of the measurements. Thus we believe that the difference between the relative variations of $d\omega_o/dT$ and $d\omega_r/dT$ can be neglected in our case.

13. N. Ono, K. Kitamura, K. Nakajima, Y. Shimanuki "Measurement of Young's modulus of silicon single crystal at high temperature and its dependence on boron concentration using the flexural vibration method" Jpn. J. Appl. Phys. 2000, 39, 368-371.
14. The results presented in Figure 2 correspond to the temperature dependence of the elastic modulus of the B-doped Si (resistivity 10 Ohm.cm) in the (100) direction, which is a typical orientation of the AFM probe. The impact of doping on the temperature behavior of the elastic modulus was found to be very small[13] and can be safely ignored.
15. S.A. Prokhorova, S.S. Sheiko, M. Moeller, C.-H. Ahn, V. Percec "Molecular imaging of monodendron jacketed linear polymers by scanning force microscopy" Macromol. Rapid Commun. 1998, 19, 359-366.
16. S.N. Magonov, "Visualization of polymers at surfaces and interfaces with atomic force microscopy" in Handbook of Surfaces and Interfaces (Nalwa Ed.) submitted.
17. W. Zhou, S.Z.D. Cheng, S. Putthanarat, R.K. Eby, D.H. Reneker, B. Lotz, S.N. Magonov, E.T. Hsieh, R.G. Geerts, S.J. Palackal, G.R. Hawley, M.B. Welch "Crystallization, melting and morphology of syndiotactic polypropylene fractions. 4. *In-situ* lamellar single crystal growth and melting in different sectors" Macromolecules 2000, 33, 6861.
18. F. Dinelli, H.E. Assender, K. Kirov, O.V. Kolosov "Surface morphology and crystallinity of biaxially stretched PET films on the nanoscale" Polymer 2000, 41, 4285-4289; D.A. Ivanov, T. Pop, D. Yoon, A. Jonas "Direct space detection of order-disorder interphases at crystalline-amorphous boundaries in a semicrystalline polymer" (submitted to Polymer).
19. D.A. Ivanov, Z. Amalou, S.N. Magonov "Real time evolution of the lamellar organization of poly(ethylene terephthalate) during crystallization from the melt: high temperature AFM study" Macromolecules 2001, submitted for publication.
20. C. Basire, D.A. Ivanov "Evolution of the lamellar structure during crystallization of a semicrystalline-amorphous polymer blend: time-resolved hot-stage SPM study" Physical Review Letters, 2000, 85, 5587-5590.
21. Yu.K. Godovsky, S.N. Magonov "AFM Visualization of Morphology and Nanostructure of Ultrathin Layer of Polyethylene during Melting and Crystallization" Langmuir 2000, 16, 3549-3552; Ponomarenko S.A., Boiko N.I., Shibaev V.P., Magonov S.N. "AFM Study of Structural Organization of Carbosilane Liquid Crystalline Dendrimer" Langmuir 2000, 16, 5487-93.

About the Authors

D.A. Ivanov
Laboratoire de Physique des Polymères,
Université Libre de Bruxelles, CP223,
B-1050 Brussels, Belgium
Email: divanov@ulb.ac.be

R. Daniels, and S.N. Magonov
Veeco Instruments Inc.
112 Robin Hill Road
Santa Barbara, CA 93117
Email: rdaniels@veeco.com
smagonov@veeco.com

Solutions for a nanoscale world.

Veeco Instruments Inc.
112 Robin Hill Road
Santa Barbara, CA 93117
805-967-1400 • 1-888-24-VEECO
www.veeco.com

Veeco Probes
www.veecoprobes.com

AN45, Rev A1, 9/1/04